Mitigating suspended-sediment environmental pressure in subsea engineering through colliding turbidity currents

Alhaddad, S.M.S.; Elerian, M.F.A.I.

DOI
10.1016/j.rineng.2024.101916

Publication date
2024

Document Version
Final published version

Published in
Results in Engineering

Results in Engineering 21 (2024) 101916

Contents lists available at ScienceDirect

Results in Engineering

journal homepage: www.sciencedirect.com/journal/results-in-engineering

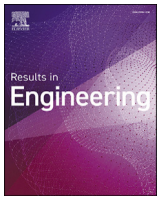

Full Length Article

Mitigating suspended-sediment environmental pressure in subsea engineering through colliding turbidity currents

Said Alhaddad *, Mohamed Elerian

Section of Offshore and Dredging Engineering, Faculty of Mechanical, Maritime and Materials Engineering, Delft University of Technology, Delft, the Netherlands

ARTICLE INFO

Keywords:
Turbidity currents
Dual-lock-exchange experiments
Dredging
Deep sea mining
Polymetallic nodules
Environmental impact

ABSTRACT

Turbidity currents have extensively been explored in quiescent environments. However, during several underwater activities (e.g., dredging and deep sea mining), generated turbidity currents could travel in opposite directions and interact with each other, which could largely influence their hydrodynamics and sediment transport capacity. Therefore, we carried out a set of dual-lock-exchange experiments to study the interaction of colliding turbidity currents. Our experimental results show that the interaction of identical currents results in the reflection of both currents with almost no mixing, forcing them to travel in the opposite direction of the pre-collision one. In contrast, when a turbidity current interacts with a lighter, less-energetic current, clear mixing is observed. Furthermore, it is revealed that the collision of turbidity currents reduces the suspended sediment transported by them, which is favorable from an environmental point of view, and slightly increases the vertical dispersion of particles. In the case of two identical counterflowing currents, a 35% reduction in mass flux, accompanied by a 6% increase in turbidity current thickness, was observed in our experiments.

1. Introduction

Turbidity currents are buoyancy-driven underflows generated by the gravity action on the density difference between a fluid-sediment mixture and the ambient fluid. These currents have extensively been studied experimentally (e.g., [20,18]) and numerically (e.g., [6,13]) in the literature in quiescent environments. However, very limited research has been carried out to investigate the interaction of turbidity currents running in opposite directions, despite the fact that this setting is encountered in subsea engineering (e.g., dredging and deep sea mining). Moreover, sedimentary deposits provide evidence of turbidity currents colliding on the ocean floor [19].

In dredging, breaching (underwater dilative slope failure) is considered an effective production mechanism, in particular for plain suction dredgers [21,2]. Breaching is typically accompanied by the generation of turbidity currents [22,14], which were investigated experimentally by Alhaddad et al. [3] and numerically by Alhaddad et al. [5]. To explain the sand mining process with a suction dredger, a real dredging activity, which took place in IJsselmeer (the Netherlands) for land reclamation, is adopted and demonstrated in Fig. 1. This dredging activity was carried out in 1968 by the Dutch company Amsterdamsche Ballast Maatschappij. The suction pipe was inserted into the sediment bed, forming very steep slopes (breach faces) around the suction mouth. As a result, the breaching process started and subsequently turbidity currents generated, which work as the carrier of sand from the breach faces to the suction mouth. The sand was sucked into the pipe and delivered to the dredger, while the steep slopes kept traveling backward in a radial direction [7]. In such an event, turbidity currents flow in opposite directions and interact eventually with each other.

Moreover, across the abyssal plains of the global ocean, polymetallic nodules are abundantly found at depths ranging from 1 km to 6 km. These nodules are tremendously rich in economically valuable metals (e.g., cobalt, copper, manganese and nickel) [12]. While mining these nodules by a hydraulic collector, sediment is inevitably picked up and collected [1]. With regard to Coandă-effect-based collectors (a category of hydraulic collectors), the sediment gathered is disposed of behind the collector, generating turbidity currents that move across the seabed [8,9]. These currents could extend over large distances, potentially causing significant disturbances to aquatic ecosystems along its path [17]. During a mining operation, several collectors will be deployed alongside each other [4], leading to the interaction of turbidity currents (see Fig. 2). Specifically, the turbidity currents moving perpendicular to the motion of the collector (referred to as sideways turbidity currents) will come into contact. A fundamental understanding of such

* Corresponding author.
E-mail addresses: S.M.S.Alhaddad@tudelft.nl (S. Alhaddad), m.f.a.i.elerian@tudelft.nl (M. Elerian).

https://doi.org/10.1016/j.rineng.2024.101916
Received 14 December 2023; Received in revised form 24 January 2024; Accepted 13 February 2024
Available online 19 February 2024

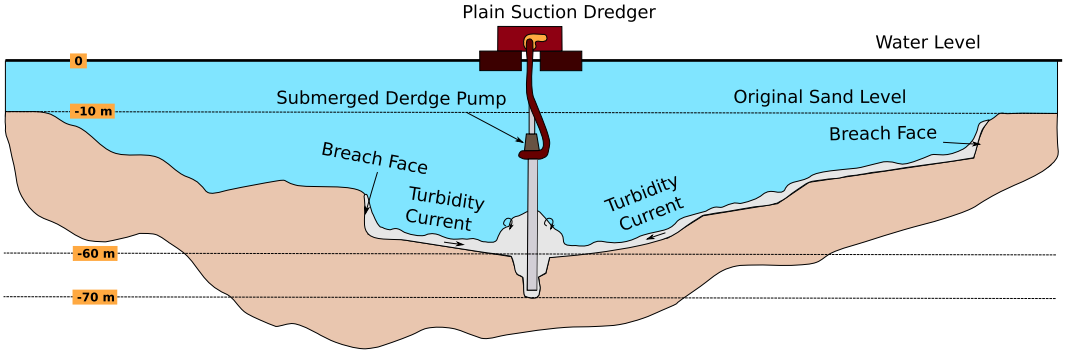

Fig. 1. Diagrammatic illustration of a real dredging activity in IJsselmeer (the Netherlands) in 1968, where turbidity currents flowing in opposite directions were encountered (modified from [23]).

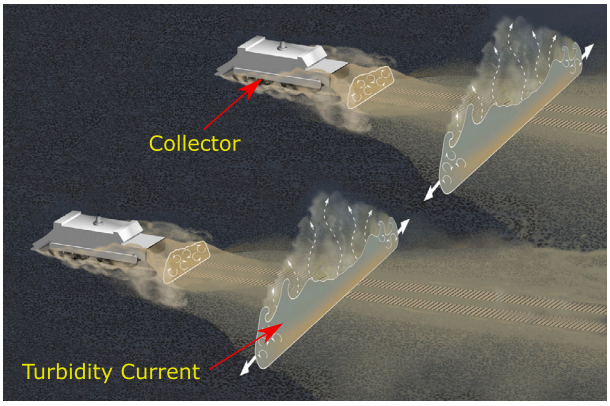

Fig. 2. Diagrammatic illustration of a couple of polymetallic nodule collectors and the turbidity currents propagating in opposite directions (modified from [16]).

an interaction is critical to improve our prediction of the evolution and fate of anthropogenic turbidity currents, which is central to the environmental impact assessment of underwater activities.

The objective of this study is to explore whether the generation of colliding turbidity currents in subsea engineering is environmentally preferred to the generation of turbidity currents running on the seabed without interaction with counterflowing turbidity currents. To this end, we conducted a series of small-scale experiments in a water flume, where a turbidity current traveling leftward and another current traveling rightward can be produced. This article presents and discusses the acquired experimental results and observations. Our experimental measurements provide the first insights into the effect of turbidity currents moving in opposing directions on each other.

2. Dual-lock-exchange experiments

The dual-lock-exchange experiment is a modified version of the classical lock-exchange experiment widely used to explore the dynamics of gravity currents. Our modified version allows for the generation of two turbidity currents flowing in opposite directions towards one another. This simple setup allows for reproducibility and easy control of initial conditions, making it well-suited for a systematic study. Additionally, it offers a clear visual representation of dynamics involved in turbidity currents.

2.1. Experimental setup

The experiments are carried out in a rectangular glass tank measuring 3 m in length (L), 0.2 m in width (W), and 0.4 m in depth (D) (see Fig. 3 and Fig. 4a). In each experiment, two locks are positioned at a horizontal distance of 0.2 m from both tank ends. To create suspensions, we used glass beads with particle sizes ranging from 0.065 mm to 0.105 mm.

Table 1
Concentration ranges and corresponding concentration increments adopted in the calibration process.

Concentration Range	Increment
0.0% - 0.1%	0.02%
0.1% - 0.2%	0.05%
0.2% - 1.0%	0.10%
1.0% - 2.0%	0.20%
2.0% - 2.6%	0.30%

To acquire detailed concentration measurements, a high-speed recording of each experiment was required. This was achieved using an 'IL5HM8512D Fastec' camera fitted with a Navitar 17 mm lens, as shown in Fig. 4d. The camera was operated at 80 frames per second. A correlation between sediment concentration and light permeability of the sediment-water mixture was established (see Subsection 2.2) and utilized to obtain the concentration for each recorded pixel. To ensure uniform lighting, a background plate equipped with white LED strips was affixed to the rear of the tank. In addition, a paper sheet is placed in front of these LED strips to create evenly-diffused light, as depicted in Fig. 4c. Furthermore, a black tent was constructed around the experimental setup, so as to create a controlled environment, where external light sources are eliminated.

2.2. Concentration calibration method

The same concentration calibration method used in the work of [10] is applied in this study. For convenience, we will briefly describe it here. The same experimental setup, comprising the tank and high-speed camera, serves the purpose of calibration as well. This calibration procedure begins by filling the right mixing chamber with fresh tap water, followed by the addition of a pre-measured mass of sediment, which is then mixed with water. After achieving the desired homogeneity in sediment concentration, a snapshot is taken of the mixing chamber. Subsequently, another pre-measured sediment quantity is introduced into the mixture and recorded. This sediment addition process continues until the resulting pixel values approach approximately 255. It is worth noting that a pixel value of 255 represents the camera's upper limit for distinguishing different shades of gray, where pixel values range from 0 for white to 255 for black (see Fig. 5). Each snapshot captures a specific concentration level. Table 1 outlines the concentration ranges and corresponding concentration increments.

2.3. Test procedure

Table 2 summarizes the initial conditions of the experiments conducted within this study. We conducted three dual-lock-exchange ex-

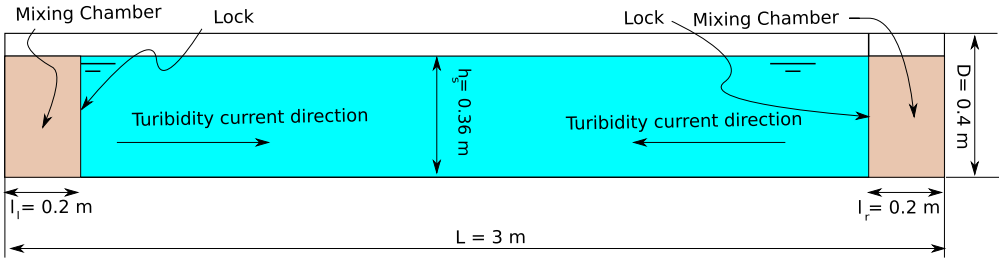

Fig. 3. Schematic front view of the dual-lock-exchange experimental setup illustrating its components.

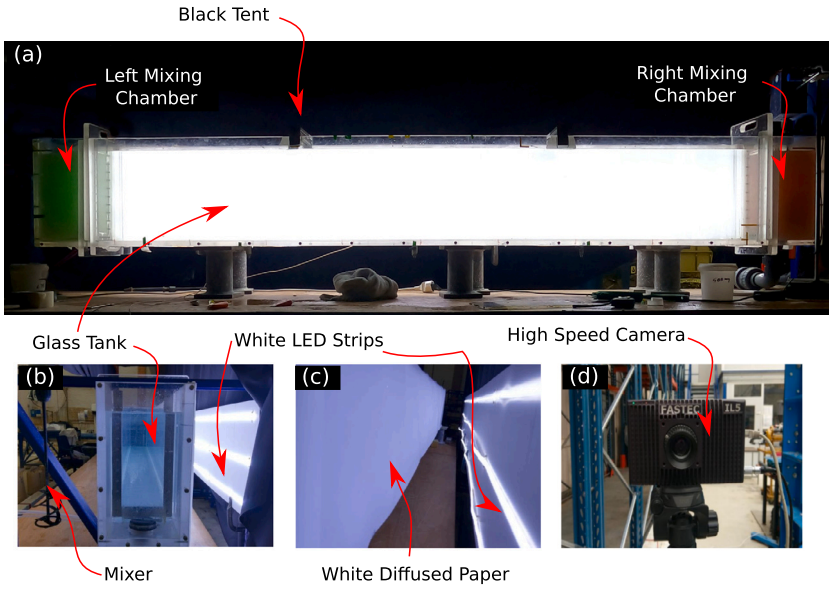

Fig. 4. Front view of the experimental setup illustrating the used tank (top). Equipment used in the experiments (bottom).

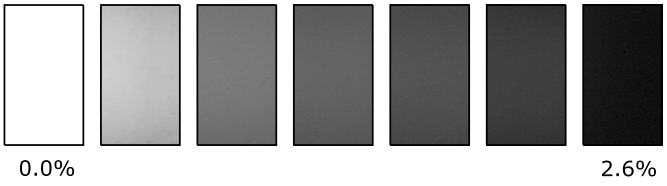

Fig. 5. Examples of snapshots taken for the concentration calibration process; sediment concentration increases from left (0.0%) to right (2.6%), with each snapshot representing a distinct concentration.

periments and one classical lock-exchange experiment with a 3%-concentration suspension as a reference case. The percentage 3% was chosen because our measuring technique can be used to retrieve concentration data up to 2.6%. It should be noted that local concentrations drop quickly below 2.6% after removing the lock, due to water entrainment. In the dual-lock-exchange experiments, we kept the sediment concentration in the right mixing chamber constant at 3%, while we varied the sediment concentration in the left mixing chamber (i.e., 1%, 2%, and 3%). Runs 2, 3 and 4 were conducted twice, during one of which dyes with different colors were added to the suspensions behind the locks, resulting in Runs 2*, 3* and 4*. These experiments were conducted to facilitate visual observation of the interaction of turbidity currents during and after collision.

In Runs 2 and 3, the sediment concentration in the mixing chambers is different, resulting in varying forward velocities for the turbidity currents after the release of locks. Consequently, the collision location of the two turbidity currents would not be in the middle of the tank. This would limit our ability to study the reflected turbidity currents due to their shorter propagation distance within the constrained tank length.

Table 2
Test matrix summarizing the experiments conducted within this study. C_l and C_r represent the volumetric sediment concentration in the left and right mixing chambers, respectively.

Run #	C_l [%]	C_r [%]	Dye Used
Run 1	0	3	No
Run 2	1	3	No
Run 3	2	3	No
Run 4	3	3	No
Run 2*	1	3	Yes
Run 3*	2	3	Yes
Run 4*	3	3	Yes

Therefore, we delayed the removal of the right lock, since the suspension behind it has the higher concentration. Runs 2 and 3 were repeated until the currents collided almost in the middle of the tank.

Every test was conducted following the next sequence of steps:

- Tank filling: Clear water is added to the experimental tank up to a height of 30 cm.
- Lock placement: The two locks are placed within the tank. In the case of a regular lock-exchange experiment, just one lock is used.
- Sediment preparation: Based on the target concentration, sediment is weighed using a digital scale and added to the mixing chambers within the tank. Following that, water is added until reaching the target water depth ($h_s = 36$ cm) everywhere in the tank.
- Mixing: Propeller-type agitators are inserted into the mixing chambers, and they are operated until a homogeneous sediment-water

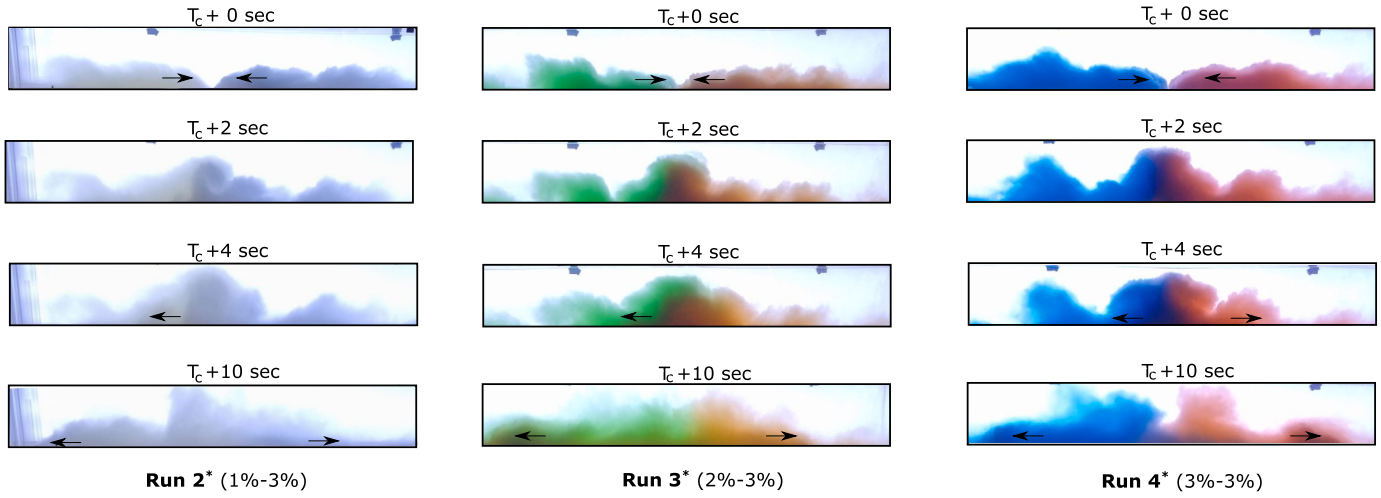

Fig. 6. Dyed experiments showing the interaction between the two turbidity currents in the three cases of interest. The arrows indicate the direction of motion and no arrows means that no horizontal motion was observed at the corresponding time. T_c is the collision time.

mixture of is achieved. This mixing process takes about 2 minutes. For flow-visualization experiments, food coloring was added to the suspensions to distinguish the denser fluids from the ambient water.

- Measurement initiation: The measurement using camera recordings is initiated to obtain the concentration distribution of turbidity currents.
- Right lock removal: The right mixer is turned off, and the right lock is released.
- Left lock removal: After a predetermined delay period, the left mixer is turned off and the left lock is released. In Run 4 and Run 4*, the left and right locks are released simultaneously.
- Measurement Termination: Measurements are stopped when one of the turbidity currents reaches the end of the tank.

3. Experimental results

3.1. General description of the results

Upon the removal of the two locks, turbidity currents generate and start flowing in the direction of the ambient water. In other words, the left suspension results in a turbidity current running rightward, while the right suspension results in a turbidity current running leftward. Given that the two currents travel in opposite directions, they meet and collide almost in the middle of the tank. As a consequence, the sediment particles are further dispersed in the vertical direction, almost reaching the water surface in Run 4.

Snapshots of the flow-visualization experiments, where food coloring was added, are depicted in Fig. 6 to illustrate the nature of the interaction and the potential mixing. In the top panels of Fig. 6 (time $= T_c$), the turbidity currents are seen just before the collision. In the next row of snapshots (time $= T_c + 2$), horizontal motion was hardly observed in the three experiments. In the case of two identical currents (Run 4*), no clear mixing between the two currents was observed. Instead, the two currents reflected back towards their starting point. Conversely, in Run 2* and Run 3*, mixing was manifestly observed; the denser current penetrated the lighter current at time $= T_c + 4$. The bottom panel of Fig. 6 (time $= T_c + 10$) shows that sediment particles from the lighter current were entrained in the denser current. Besides, in Run 2* and Run 3*, a portion of the denser current reflected back, as a result of collision.

In the following, we will analyze the turbidity currents in more detail by looking into the density fields (Fig. 7) and the amount of suspended sediment transported by the current traveling leftward after collision. Besides, we will explore the change in the thickness of turbidity currents. In this way, we investigate the influence of the interaction of currents on the current produced by the 3%-concentration suspension.

3.2. Sediment mass flux

The sediment mass flux per unit width is estimated here to investigate the effect of opposing turbidity currents on the sediment transport by turbidity currents. This estimate is assessed on a vertical interrogation plane, which is located at a distance of 90 cm from the left tank end and denoted by the dotted vertical line in Fig. 7. Assuming that the velocity of the turbidity current is uniform across its height, the sediment mass flux $\dot{m}$ [kg/m/s] can be calculated by

$$\dot{m} = U_f \int_0^{h_s} c \, \mathrm{d}z, \tag{1}$$

where U_f [m/s] is the average front speed of the turbidity current, h_s [m] is water surface height, c [kg/m^3] is the local suspended sediment concentration and z [m] is the upward-normal coordinate. In our calculations, the front speed U_f was averaged over the time frame of analysis (7 seconds corresponding to the density fields shown in Fig. 7). This period was chosen because it was not long enough for the currents traveling leftward to reach the left flume end and thus reflect. The temporal change of the sediment mass flux passing the interrogation plane over the selected 7 seconds is shown in Fig. 8. It is worth noting that the difference in the sediment mass flux between the cases is completely attributed to the difference in sediment concentration ($U_f = 10$ cm/s was found to be similar in all cases).

Fig. 8 depicts that the sediment mass flux peaked shortly after the head of the current had passed the interrogation plane. This peak was the largest when there was no turbidity current incident on the current traveling leftward. In contrast, the peak was the smallest in the case of two identical currents. This is attributed to the fact that no clear mixing was observed between the two currents, as they are equal in density and velocity; they collide in the middle of the tank and force each other to reflect back towards their initial departure point (see Fig. 6 right). The second largest peak was for Run 3 where the denser current collided and mixed with the lighter current. Collision of currents results in vertical dispersion of particles, while mixing results in particle entertainment from the lighter current into the denser current. The lighter current in Run 3 has a higher concentration than the lighter current in Run 2, explaining why the peak was larger in Run 3. In other words, more particles were intruded into the denser current in Run 3.

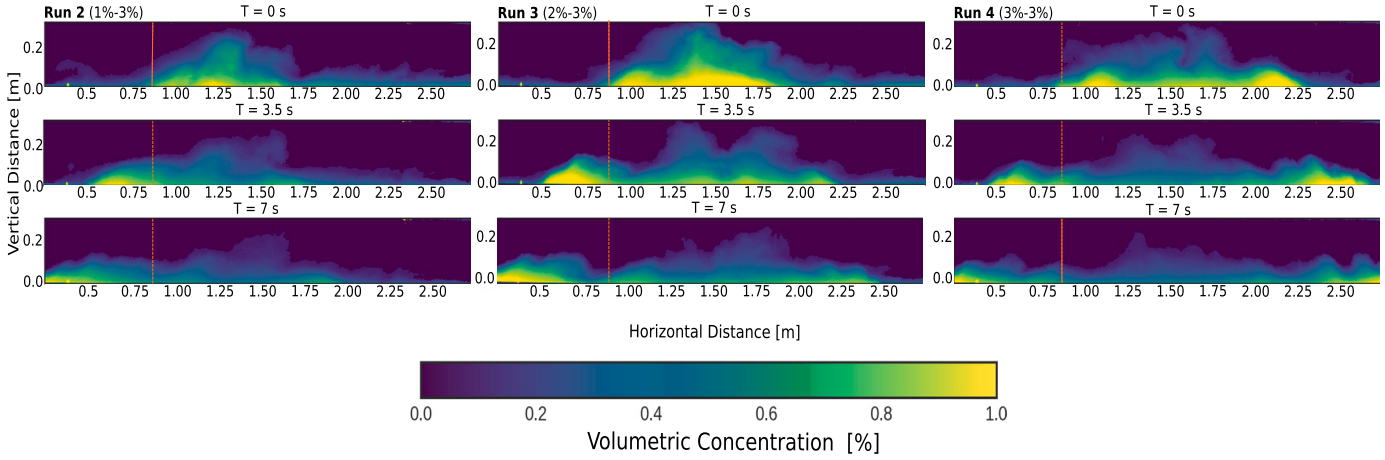

Fig. 7. Volumetric concentration maps of the turbidity currents at three different time instances. $T = 0$ is the time at which the currents propagating leftward after collision reach the interrogation plane (indicated by the vertical dashed line). From left to right, the cases are 1%-3%, 2%-3% and 3%-3%, respectively.

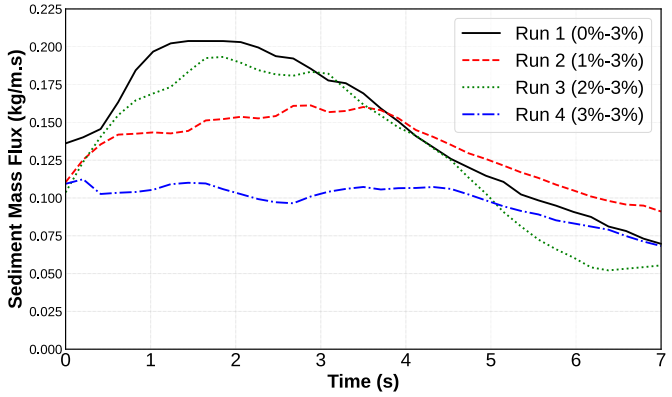

Fig. 8. Temporal change of the sediment mass flux passing the interrogation plane. $T = 0$ is the time at which the currents propagating leftward reach the interrogation plane.

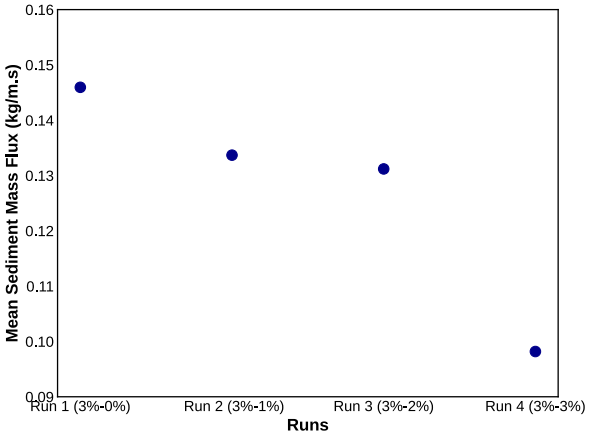

Fig. 9. Sediment mass flux averaged over a 7-second time span for the cases shown in Fig. 8.

Fig. 9 clearly shows that the average sediment mass flux decreases as the density of the opposing current increases. Compared with the case with no incident current (Run 1), the average sediment mass was suppressed by nearly 35% in Run 4. The difference between the average sediment mass flux for Run 2 and Run 3 is small (Fig. 9), although the lighter current was completely entrained into the denser current in both experimental runs, as shown in Fig. 6. This is attributed to the fact that a smaller portion of the particles originally belonging to the

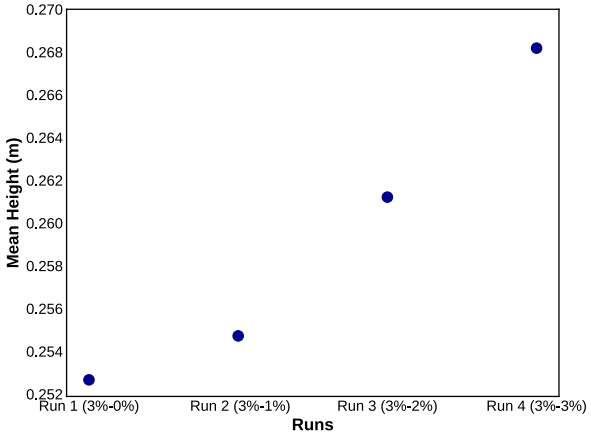

Fig. 10. Thickness of current averaged over a 7-second time span for the cases shown in Fig. 8.

denser current reflected back in Run 2, in comparison with Run 3. This can clearly be seen in the concentration maps presented in the left and middle panels of Fig. 7.

3.3. Thickness of turbidity current

The thickness of the turbidity current at the interrogation plane can be estimated as:

$$H = \frac{\int_0^{h_s} cz\,\mathrm{d}z}{\int_0^{h_s} c\,\mathrm{d}z}. \tag{2}$$

The average turbidity current thickness over the selected duration (7 seconds) for all cases is presented in Fig. 10. Although the differences in thickness are not large, a clear trend can be observed, which is opposite to the trend of the average sediment mass flux. For instance, compared with the case with no incident current (Run 1), the average thickness was increased by 6% in Run 4. This suggests that the interaction of opposing currents leads to more vertical dispersion of particles.

4. Discussion

The presence of suspended sediment reduces light penetration into water, consequently decreasing the amount of light available to seabed photosynthesizers. Besides, the suspended sediment could eventually settle out on sensitive marine plants and creatures (i.e., fish, coral reefs and seagrass beds), possibly smothering them. Turbidity currents

represent an important agent of sediment transport in submarine environments [15] and the generation of these currents during underwater engineering activities can be inevitable.

The findings of this study suggest that the generation of colliding turbidity currents in subsea engineering is environmentally preferred to the generation of turbidity currents propagating on the seabed without interaction with counterflowing turbidity currents. This is primarily because of the reduction of the sediment mass flux and thus the associated environmental stress [8]. By reducing sediment mass flux, water turbidity decreases, sediment deposition on aquatic ecosystems decreases, and the intensity of sediment resuspension events can be decreased. This implies that having several Coandă-effect-based collectors mining next to each other is a potential approach to reduce the corresponding environmental impact. Other underwater activities (i.e., dredging and underwater slope construction) may also be designed in a way that results in the collision of turbidity currents.

In our study we used a two-dimensional lock-exchange configuration, where turbidity currents cannot spread in the lateral direction. Therefore, conducting field measurements would facilitate a better comparison between the mechanisms observed in the laboratory and those occurring in the field. In the future, we plan to extend this study by looking into a wider range of sediment concentrations and by using a longer water flume where more spatio-temporal data can be acquired.

The collision of turbidity currents enhances mixing and thus the likelihood of particles colliding with each other. In the case of cohesive sediment, mixing triggers a flocculation effect, leading to the formation of flocs that settle out faster than individual particles [11]. Consequently, the buoyancy-driven forces of the current will decrease, which will further dampen it [9]. In this context, we also plan to test cohesive sediment to investigate the impact of colliding currents on the probability of floc formation.

5. Conclusions

To mainly explore the environmental implication of producing colliding turbidity currents, we carried out a series of dual-lock-exchange experiments. The experimental results showed that turbidity currents traveling in opposite directions with identical dynamics hardly mix; their collision results in further dispersion of their sediment particles in the vertical direction at the collision phase followed by a reflection of the two currents. Conversely, when the density of the two opposing currents is different, mixing clearly occurs and the lighter current intrudes into the denser current. Depending on the density of the lighter current, a portion of the sediment of the denser current may reflect back as a result of the interaction. Our study reveals that the collision of turbidity currents reduces the amount of suspended sediment transported by them, which is favorable from an environmental point of view, while it slightly increases the turbidity current thickness. Specifically, the mass flux was reduced by 35%, while the turbidity current thickness increased by 6% in the case of two identical counterflowing currents.

Notation

c	Local suspended sediment concentration	-
H	Thickness of the turbidity current	m
h_s	Water surface height	m
$\dot{m}$	Sediment mass flux	kg/m/s
T	Time	s
T_c	Collision time	s
U_f	Average front speed of the turbidity current	m/s
z	Upward-normal coordinate	m

CRediT authorship contribution statement

Said Alhaddad: Writing – review & editing, Writing – original draft, Visualization, Supervision, Methodology, Investigation, Formal analysis, Data curation, Conceptualization. **Mohamed Elerian:** Writing – original draft, Visualization, Software, Methodology, Investigation, Formal analysis, Data curation, Conceptualization.

Declaration of competing interest

The authors declare that they have no known competing financial interests or personal relationships that could have appeared to influence the work reported in this paper.

Data availability

Data will be made available on request.

Acknowledgement

The authors would like to thank the group of Mechanical Engineering bachelor students at Delft University of Technology that conducted the laboratory experiments used in this study.

References

[1] S. Alhaddad, R. Helmons, Sediment erosion generated by a coandă-effect-based polymetallic-nodule collector, J. Mar. Sci. Eng. 11 (2023) 349.
[2] S. Alhaddad, R.J. Labeur, W. Uijttewaal, Breaching flow slides and the associated turbidity current, J. Mar. Sci. Eng. 8 (2020) 67.
[3] S. Alhaddad, R.J. Labeur, W. Uijttewaal, Large-scale experiments on breaching flow slides and the associated turbidity current, J. Geophys. Res., Earth Surf. (2020).
[4] S. Alhaddad, D. Mehta, R. Helmons, Mining of deep-seabed nodules using a coandă-effect-based collector, Results Eng. 17 (2023) 100852.
[5] S. Alhaddad, L. de Wit, R.J. Labeur, W. Uijttewaal, Modeling of breaching-generated turbidity currents using large eddy simulation, J. Mar. Sci. Eng. 8 (2020) 728.
[6] E. Biegert, B. Vowinckel, R. Ouillon, E. Meiburg, High-resolution simulations of turbidity currents, Prog. Earth Planet. Sci. 4 (2017) 1–13.
[7] J. De Koning, Developments in hydraulic deep dredging, in: Proceedings of the Latin American Dredging Congress, Mexico-City, April 1981, pp. 5–10.
[8] M. Elerian, S. Alhaddad, R. Helmons, C. van Rhee, Near-field analysis of turbidity flows generated by polymetallic nodule mining tools, Mining 1 (2021) 251–278.
[9] M. Elerian, Z. Huang, C. van Rhee, R. Helmons, Flocculation effect on turbidity flows generated by deep-sea mining: a numerical study, Ocean Eng. 277 (2023) 114250.
[10] M. Elerian, C. Van Rhee, R. Helmons, Experimental and numerical modelling of deep-sea-mining-generated turbidity currents, Minerals 12 (2022) 558.
[11] B. Gillard, K. Purkiani, D. Chatzievangelou, A. Vink, M.H. Iversen, L. Thomsen, Physical and hydrodynamic properties of deep sea mining-generated, abyssal sediment plumes in the clarion clipperton fracture zone (eastern-central Pacific), Elem. Sci. Anth. 7 (2019) 5.
[12] J.R. Hein, A. Koschinsky, T. Kuhn, Deep-ocean polymetallic nodules as a resource for critical materials, Nat. Rev. Earth Environ. 1 (2020) 158–169.
[13] L.V. Lucchese, L.R. Monteiro, E.B.C. Schettini, J.H. Silvestrini, Direct numerical simulations of turbidity currents with evolutive deposit method, considering topography updates during the simulation, Comput. Geosci. 133 (2019) 104306.
[14] D.R. Mastbergen, J.H. Van Den Berg, Breaching in fine sands and the generation of sustained turbidity currents in submarine canyons, Sedimentology 50 (2003) 625–637.
[15] E. Meiburg, B. Kneller, Turbidity currents and their deposits, Annu. Rev. Fluid Mech. 42 (2010) 135–156.
[16] C. Muñoz-Royo, R. Ouillon, S. El Mousadik, M.H. Alford, T. Peacock, An in situ study of abyssal turbidity-current sediment plumes generated by a deep seabed polymetallic nodule mining preprototype collector vehicle, Sci. Adv. 8 (2022) eabn1219.
[17] T. Peacock, R. Ouillon, The fluid mechanics of deep-sea mining, Annu. Rev. Fluid Mech. 55 (2022).
[18] O.E. Sequeiros, R. Mosquera, F. Pedocchi, Internal structure of a self-accelerating turbidity current, J. Geophys. Res., Oceans 123 (2018) 6260–6276.
[19] J.E. Simpson, Gravity Currents, 2nd edition, Cambridge University Press, 1997.
[20] M. Stagnaro, M.B. Pittaluga, Velocity and concentration profiles of saline and turbidity currents flowing in a straight channel under quasi-uniform conditions, Earth Surf. Dyn. 2 (2014) 167.
[21] J.H. Van Den Berg, A. Van Gelder, D.R. Mastbergen, The importance of breaching as a mechanism of subaqueous slope failure in fine sand, Sedimentology 49 (2002) 81–95.
[22] C. Van Rhee, A. Bezuijen, The breaching of sand investigated in large-scale model tests, in: Coastal Engineering, 1998, pp. 2509–2519.
[23] W. Vlasblom, Lecture Notes of Dredging Processes, Delft University of Technology, 2003.